FRINGE 96
On the Interferometric Coherence: A Multifrequency and Multitemporal Analysis

K.P. Papathanassiou	DLR Oberpfaffenhofen, P.O. Box 1116, D-82230 Wessling, Germany papathanassiou@dlr.de
A. Reigber	DLR Oberpfaffenhofen, P.O. Box 1116, D-82230 Wessling, Germany reigber@ohffo1.hf.op.dlr.de
M. Coltelli	Instituto Internazionale di Vulcanologia, Piazza Roma 2, I-95123 Catania, Italy colt@iiv.ct.cnr.it

Abstract

The potential of satellite repeat-pass SAR interferometry for mapping and monitoring of different natural surfaces is discussed here. The presented approaches are based on analysis of the interferometric coherence using SIR-C/X-SAR and ERS-1/ERS-2 tandem data from the Mt. Etna test site in Sicily, Italy. The evaluation of the frequency dependent coherence of several volcanic terrain types is used as a first order approach for classification. Parallel a second classification algorithm based on the temporal decorrelation behavior of different surfaces in only one frequency is addressed. The results of the algorithms are compared and discussed.

Keywords: SAR interferometry, coherence analysis, multitemporal classification, multifrequency classification

1. Introduction

The illumination of the same area with two antennas with slightly different look angles leads to the assumption that the statistical phase contribution due to the different speckle characteristic in the two received signals is about the same. Their phase difference is therefore deterministic and corresponds to the path difference of both signals. The interferometric coherence is defined as the normalized complex cross-correlation of both complex signals s_1 and s_2:

$$\gamma = \frac{< s_1 s_2^* >}{\sqrt{< s_1 s_1^* >< s_2 s_2^* >}}$$

where <...> means the expectation value and * is the complex conjugation operator. The absolute value of the interferometric coherence varies between 0 and 1. The coherence is a maximum if both signals are identical, and vanish if the signals do not correlate. Interferometric coherence depends primarily on:

Baseline: the spatial separation of the two antennas has to be smaller than the critical effective baseline. The loss of coherence due to the non-overlapping parts of the range spectra can be avoided by applying range spectral filtering. [1] [2]
Doppler centroid: the azimuth doppler spectra of the two passes must have sufficient overlap, i.e. the two surveys must see the scene under the same squint angle. Also here, the decorrelation due to the only partial overlap of the azimuth spectra can be filtered. [3] [4]
Additive noise in either signal, processing artifacts and defocusing.

If the two signals are not received simultaneously (one-pass interferometry) but at different times during two repeating passes over the same area (repeat-pass interferometry) the following additional temporal decorrelation effects decrease the coherence:

changing of the scattering geometry within the resolution cell during the time between the two aquisitions,
changing of the physical properties of the scattering mechanisms during the time between the two aquisitions,
changing of the behaviour of the propagation medium (atmospheric effects).

The amount of temporal decorrelation describes processes occurring on size scales of the signal wavelength with a time resolution defined by the repeat time interval (temporal baseline). The sensitivity of the coherence to changes in the characteristics of the scattering mechanisms in time can be used for the detection of a wide variety of surface processes and the corresponding surface types.

2. Data description and processing

For the presented investigations data aquired during the second SIR-C/X-SAR mission and ERS-1/ERS-2 tandem data of the Mt. Etna Sicily/Italy test site were used. This test site has been choosen because of the availability of good geological and topographic maps as well as an interferometric and photogrammetric DEM. The multifrequent SIR-C/X-SAR data sets were acquired on October 9 and 10, 1994 (data takes 141.1 and 157.1). The C- and L-band image pairs were processed by NASA/JPL in Pasadena, and the X-band image pair was processed by DLR/D-PAF in Oberpfaffenhofen. The multitemporal ERS-1/ERS-2 data sets were aquired on September 5-6 and on November 14-15, 1995 (frame 0747) and processed by DLR/NE-HF in Oberpfaffenhofen [5].

After spectral filtering in range and azimuth of the SLC images and coregistration we form the interferogram by multiplying the first image with the complex conjugate of the second image. The coherence images are evaluated using an average window with a size of 4 (range) by 5 (azimuth) pixels for the SIR-C/X-SAR data and of 4 by 12 pixels for the ERS-1/ERS-2 data. Because of this big average window the bias in the coherence estimation is small and has been neglected [6].. To avoid the influence of topography in the coherence estimation, we have extracted the topography related phase-gradient from the interferogram before the coherence estimation.

3. Multifrequency coherence analysis

Figure 3 shows the slant-range coherence maps of the Etna test site in the three frequencies, aquired with a time difference of one day between the pictures. White corresponds to a coherence of 1, and black corresponds to a coherence of 0.

3.1. Interpretation of the coherence maps

Lava flows around the volcano, where no or only pioneer vegetation is present, show a high temporal stability and have high coherence in all three frequencies. Very young lava on the eastern side of the volcano has a higher coherence in X-band than in C- and L-band. The reason for this effect could be the high scattering sensitivity of the short wavelength for the small scale roughness component, characteristic for young lava surfaces [7]. The high backscattered intensity in X-band increases the signal-to-noise ratio of the received signal and the resulting coherence values are therefore higher compared with the corresponding values in the C- and L- band coherence maps.

On the eastern side of the volcano a triangular feature having a very low coherence can be seen in the L-band coherence map below the three craters. This feature corresponds to an area covered with fresh volcanic fallout. The fact of volume scattering alone is not enough to justify such a high decorrelation, so it can be assumed that a change in the volume-scattering properties has occurred during the time between the two

passes, e.g. a change in the volume moisture content. Unfortunately, it was not possible to get detailed information about weather conditions during the mission to verify this assumption.

We can also see that the forested areas around the volcano are dark in X- and C-bands and bright in L-band. The reason for this is that short wavelengths like X-band and C-band do not penetrate into the forest volume, and the backscattering from branches and leaves on the top of the trees is dominant. The movement of the tree branches produces a change in the scatterer geometry inside a resolution cell and therefore, a degradation in the coherence between the two interferometric images. In L-band the waves penetrate into the forest volume, and the backscattering is mainly due to double bounce and surface scattering. Therefore, the influence of the scatterer movement in the upper part of the trees is neglectible, and the coherence is high. The same is valid for agricultural areas around settlements. The settlements, however, have a high coherence in all three frequencies as expected.

3.2. Multifrequency classification

Based on the interpretation of the frequency dependent behavior of the interferometric coherence mentioned in the previous section a first-order classification algorithm is addressed. A schematic representation of this algorithm is shown in Figure 1. The starting frequency for the classification is X-band because this frequency shows a higher sensitivity in its interaction with different surface textures. Four different classes of surface, each having different coherence values and characterized by homogeneous geological and/or morphological properties, were detected:

Class A: Surfaces with a coherence below 0.40. This class contains surfaces of high and dense vegetation such as the pine and oak forests and tree plantations around the volcano, but also a part of the fresh ash and scoria mantle that covers the upper region of Etna, in particular the scoria fallout deposit from the 1990's eruptions. In Figure 4a this class is indicated with dark green.
Class B: Surfaces with a coherence between 0.40 and 0.55. This class represents surfaces with lower vegetation as bushes, meadows, grasses, and agricultural growings, and also the ash and scoria mantle with pioneer vegetation, most of the ash and scoria mantle without vegetation, and the summit craters of Etna with fumaroles, lateral scoria cones, and very old lava (>15.000 years) with intermittent ash cover. In Figure 4a this class is indicated with dark grey.
Class C: Surfaces with a coherence between 0.55 and 0.65. This class includes historical lava flows with alterated surface, historical lava flows with pioneer vegetation, historical lava with ash cover, a few prehistorical lava, and buildings and other man-made structures. In Figure 4a this class is indicated with yellow.
Class D: Surfaces with a coherence between 0.65 and 1.0. This class consists off historical lava flow with fresh surfaces (most of these are less than three centuries old) and a few prehistorical lava with fresh surfaces (less than 3000 years). In Figure 4a this class is indicated with orange.

A very good discrimination can be made in X-band between lava surfaces and the other surface types. Also the discrimination between high and low vegetation is very successful. However, the coherence behaviour of surfaces covered with fresh ash or fresh scoria and high vegetation, and the coherence behaviour of the older ash or scoria mantle and lower vegetation are too similar for discrimination with only one frequency. Further ambiguities are present in the differentiation of prehistorical and historical lava covered with ash and/or pioneer vegetation. For the elimination of these ambiguities it is necessary to extract information from the other two frequencies:

The coherence difference between X- and C-band can be used for evaluation of the ambiguities of the different lava surface types. Lava surfaces covered with pioneer vegetation have a higher coherence in C-band than in X-band. On the other hand, lava without vegetation or ash cover and with very fresh surface has a higher coherence in X-band than in C-band. In this way it is possible to split the last two classes into new, thematic more restricted and homogeneous classes.
The coherence difference between C- and L-band reaches a maximum for surfaces with vegetation due to the different scattering mechanisms of these two frequencies. Using the coherence difference between C- and L-band, a separation of surfaces with vegetation from surfaces covered with ash and scoria can be made.

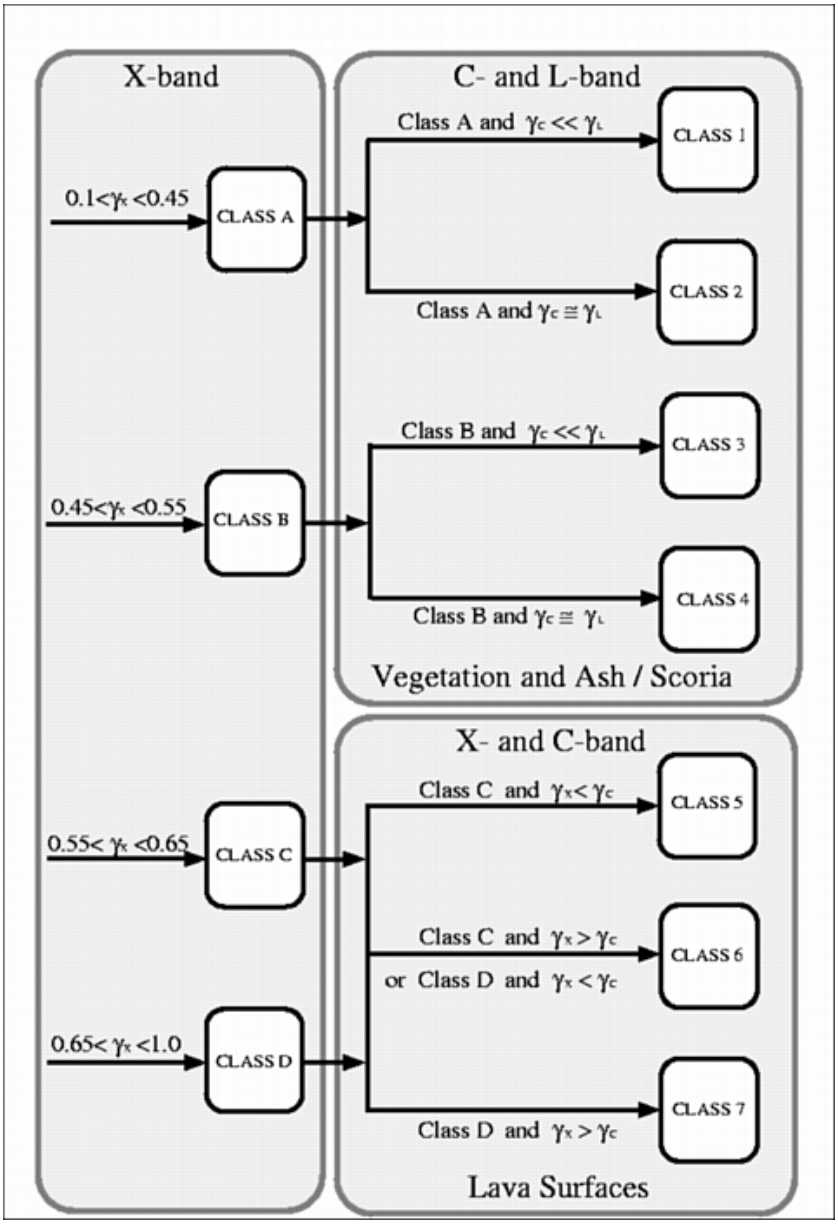

Figure 1: Multifrequency coherence classification algorithm scheme.

The result of classifying the coherence differences in the three frequencies is given in the following seven classes:

Class 1: Surfaces with a coherence below 0.40 in X-band and with a high coherence difference between C- and L-band. This class contains now mainly surfaces of high and dense vegetation. The small part of the ash and scoria fallout deposit of the 1990's eruptions of Etna that is included in this class can by considered as an error due to the low coherence of L-band in this region. In Figure 4b this class is indicated with dark green.
Class 2: Surfaces with a coherence between 0.10 and 0.40 in X-band and with a low coherence difference between C- and L-band. This class consists off the majority of the ash and scoria fallout of the 1990's eruptions, and a part of the summit craters with fumaroles. In Figure 4b this class is indicated with pale grey.
Class 3:Surfaces with a coherence between 0.40 and 0.55 in X-band and with a high coherence difference between C- and L-band. This class includes mainly surfaces with lower vegetation, and agricultural areas, as well as parts of the old ash and scoria mantle covered with pioneer vegetation. This class is indicated with pale green.
Class 4: Surfaces with a coherence between 0.40 and 0.55 in X-band and with a low coherence difference between C- and L-band. This class contains the majority of the ash and scoria mantle without vegetation, lateral scoria cones, and very old lava with intermittend ash cover. In Figure 4b this class is indicated with dark grey.
Class 5: Surfaces with a coherence between 0.55 and 0.65 in X-band and with a lower coherence in X-band than in C-band. This class includes historical lava flow with alterated surface and historical lava flow with ash and/or pioneer vegetation cover. This class is indicated with yellow.
Class 6: Surfaces with a coherence between 0.55 and 0.65 in X-band and a higher coherence in X-band than in C-band, or with a coherence between 0.65 and 1.0 in X-band and a lower coherence in X-band than in C-band. In this class are mainly historical lava flows and a few prehistorical lava with fresh surfaces. In Figure 4b this class is indicated with orange.
Class 7: Surfaces with a coherence between 0.65 and 1.0 in X-band and with a higher coherence in X-band than in C-band. In this class we find only very young lava flows. In Figure 4b this class is indicated with red.

3.3. Error analysis

In order to provide a quality assessment of the classification algorithm it is appropriate to measure quantitatively how good the classification results matches the volcanic terrain. A way to accomplish this is to compare the classification results to the available geological maps. This caused some problems due to the different scales and thematic contents in coherence and geological maps.

Class 2 falls within the 5 January 1990 scoria fall deposit typology, and the classification error is about 10% mainly due to the large dark green triangle in Fig. 3 located SW of the summit craters, which, due to the presence of sparse vegetation, coming out from the scoria deposit, belongs to class 1.

With regard to class 4, we note that the expected typologies are the summit and adventive pyroclastics cones and the older lava, depending on the amount of ageing of the different areas. The classification error is about 12%, because in the lower regions this kind of typology is covered by vegetation and frequently falls into classes 1 and 3.

Since classes 5 and 6 corresponds to the same typology of historical lava flows, only a overall performance analysis can be accomplished. The classification error is around 10%. Several historical lava flows, expected in class 5, are classified in the class 4 due to growth of the vegetation (in particular on the lower flanks of the volcano).

For the classes 1 and 3, including the vegetated areas, it was not possible to find accurate and actual botanic maps of the area to check the accuracy of the separation. Analysis based on selected areas show that the classification error between high and dense and sparce vegetation is around 20%. On the other hand the separation between vegetated and unvegetated surfaces is very high (>95%).

4. Multitemporal coherence analysis

In order to reduce the statistical errors in the coherence estimation and the influence of occasionally local effects we have calculated a mean value between the two one-day maps from the September and November data, and also from the ERS-1/ERS-1 and the ERS-2/ERS-2 constellation with 70 days time difference. Figure 5 shows the resulting two slant-range coherence maps.

Due to the very montainous region with terrain heights between 0 and 3400 meters and the very steep sensor look angle of 22 degrees the coherence maps show strong geometrical deformations, especially on the western side of the volcano. Locally very high slopes are causing either layover areas or are distorting the picture so strong that it is not possible to recognize the features of the coherence map. It is very complicated to make any prediction there. In the following we therefore concentrate only on the eastern side of the volcano.

4.1 Interpretation of the coherence maps

In an elliptic region around the top the coherence is very low in the tandem pair from November and also in both 70-days pairs. The snow line on Etna at the november, 15th 1995 was around 2400m, which corresponds very well with the observed low coherent area. The low coherence in this area does not allow a further classification.

The young and uncovered lava flows around the volcano show a very high coherence in the 1-day and also in the 70-days map. As it could be expected, the temporal stability is very high on this rocky ground. All other surfaces show an essentially higher decorrelation in time. Older lava fields, which are already covered with pioneer vegetation or with some sporadic bushes, show a decrease in the coherence, but even after 70 days they are clearly visible in the coherence map. The highly correlated backscattering from the bare lava surfaces between the vegetation causes this high long-time coherence. Also the settlements and other man-made structures show this kind of stability. The denser vegetation of various height which grows on old, earthy ground, is totally uncorrelated after 70 days and appears black in the correspondig map. But in this regions the short-time coherence allows a separation of the different land covers. High and dense vegetation like forests show a very low coherence even in the 1-day map, mostly because of the movements of the leaves and branches. Lower vegetation is more correlated, especially meadows and harvested agricultural fields have a very high coherence which produces ambiguities with lava surfaces if one only looks at the 1-day coherence.

4.2. Multitemporal classification

Based on the interpretation of the time dependent decay of the coherence in only one band as mentioned in the previous section, a first order classification algorithm has been developed. The snow-covered area around the top has been masked out by hand. A schematic representation of this algorithm is shown in Figure 2. We started with the 70-days coherence map with the intention to extract all lava and man-made surfaces. We are able to detect the following homogenous surfaces:

> **Class A: Surfaces with a long-time coherence over 0.70.** This class contains all the historical and some of the prehistorical lava flows with fresh surfaces.
> **Class B: Surfaces with a long-time coherence between 0.40 and 0.70.** This class contains mainly old lavaflows in lower regions which are again sporadic vegetated with bushes and other low vegetation. We also find settlements and other man-made structures in this class.
> **Class C: Surfaces with a long-time coherence below 0.40.** In this class we find all surfaces which are completly covered with vegetation of different height.

With the long-time coherence a very good discrimination can be made between mostly uncovered areas with rocky ground and surfaces with vegetation. Also the discrimination between fresh lava surfaces and older, slightly vegetated lava is sucessfull. All the completely vegetated surfaces appear decorrelated in the long-time coherence. To classify these areas it is possible to use the short-time coherence. The lava surfaces are already separated so no ambiguities between lava and other high coherent areas can occur. The result of this classification is shown in Figure 6

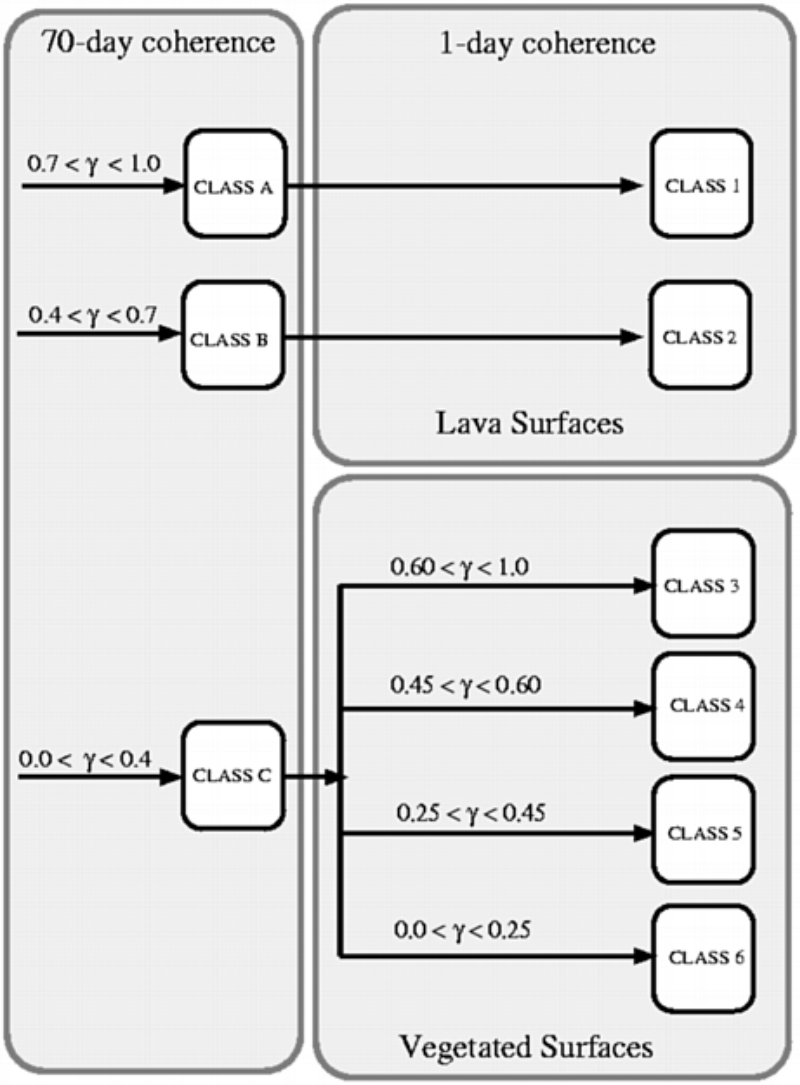

Figure 2: Multitemporal coherence classification algorithm scheme.

With this method we were able to detect following six different classes:

Class 1: Surfaces with a 70-days coherence over 0.70. This class, in Figure 6 shown in yellow, remains the same as before. It contains all the historical and some of the prehistorical lava flows with fresh surfaces.
Class 2: Surfaces with a 70-days coherence between 0.40 and 0.70. Also this class remains the same as before and contains mainly old lavaflows which are sporadically vegetated and man-made structures. This class is indicated with purple.
Class 3: Surfaces with low long-time coherence and a 1-day coherence over 0.60. In this class we find low meadows, actually unvegetated cultivated areas and other surfaces with very low vegetation and is indicated with pale green in figure 6.
Class 4: Surfaces with low long-time coherence and a 1-day coherence between 0.45 and 0.60. This class shown in green consists of lower vegetation like bushes and vineyards as well as ash and scoria mantle without vegetation. This class is indicated with green
Class 5: Surfaces with low long-time coherence and a 1-day coherence between 0.25 and 0.45. This class contains mainly surfaces with high and dense vegetation, like pine and oak forest and is shown in dark green in figure 6
Class 6: Surfaces with low long-time coherence and a 1-day coherence below 0.25. This class contains only the water of the mediterraniean sea, which appears fully decorrelated. In the case of presence of very dense forest a misclassification of the forest into this class could happen. This class is indicated with blue

4.2. Error analysis

Like in section 3.3 we compared the obtained results with the geological and also with the topographic map. Geometrical errors in the coherence maps and the low information about the vegetation complicated the error analysis in some cases.

Class 1 corresponds very well to the historical lava flows around the volcano. The classification error is about 15%, mainly due to high regions which are partly covered with fresh ash or pyroclastic material. In this case a misclassification into class 2 could happen. Except for this case, the recognition of lava with sporadic vegetation is very successful. The error in the separation of this kind of vegetation from other vegetated surfaces is around 7%. The completely ash covered lava in the higher regions which also appear in class 4 show an error of about 10%, mostly because partly covered lava sometimes shows also a fast decorrelation.

For the classes 3,4 and 5, which include the dense vegetation on earthy ground, it was not possible to find actual and accurate enough botanic maps of the area to check the accuracy of the separation. Analysis based on selected areas show that the classification error between high and dense and lower vegetation is around 15%. The error in the separation of lower vegetation and meadows and bare soil is around 20%. In any case it is not easy to divide some vegetation types into a special class.

5. Conclusions

As the obtained results show, the INSAR coherence can be used as a potential tool for the classification of different natural surfaces. The advantage of the coherence classification is the high sensitivity in the detection of temporal changes. The main problem is to relate the detected changes with a certain surface type or scattering mechanism. This relation is not in any case unambiguous because the same amount of change can be the result of different change processes. From this point of view a priori information can increase drastically the accuracy of the classification results.

The separation of vegetated areas from non-vegetated areas could be done very accurate with a short wavelength like X- or C- band and a temporal offset of one day. For further information it is very useful to use either several frequencies or multiple temporal offsets.

The multifrequency classification shows a high sensibility on unvegetated surfaces, because the different wavelengths offer the possibility to detect changing processes occuring on different orders of magnitude. Also the different penetration capabilities of the frequencies allow a better localisation and interpretation of the changing mechanisms.

In contrast the multitemporal approach is more successful in the separation of different vegetated surfaces. It takes advantage of the different time scales in the change processes of the vegetation, which can be well obsereved with a short wavelenght. To get more instructive informations it would be helpful to observe better distributed temporal offsets than the tandem data could provide.

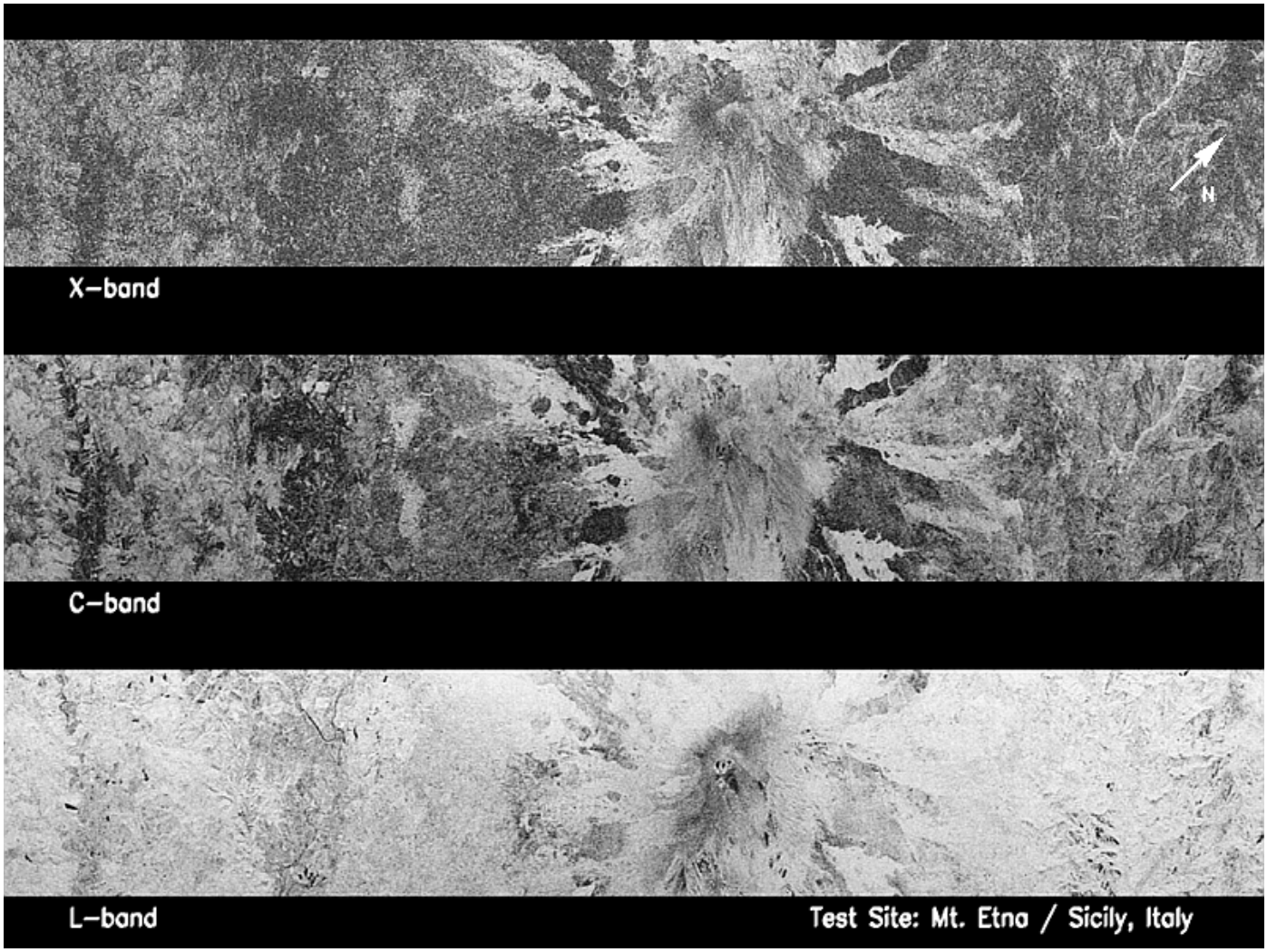

Figure 3: Coherence maps of the Mt. Etna area in the three frequencies: X- (left), C- (middle) and L-band (right).

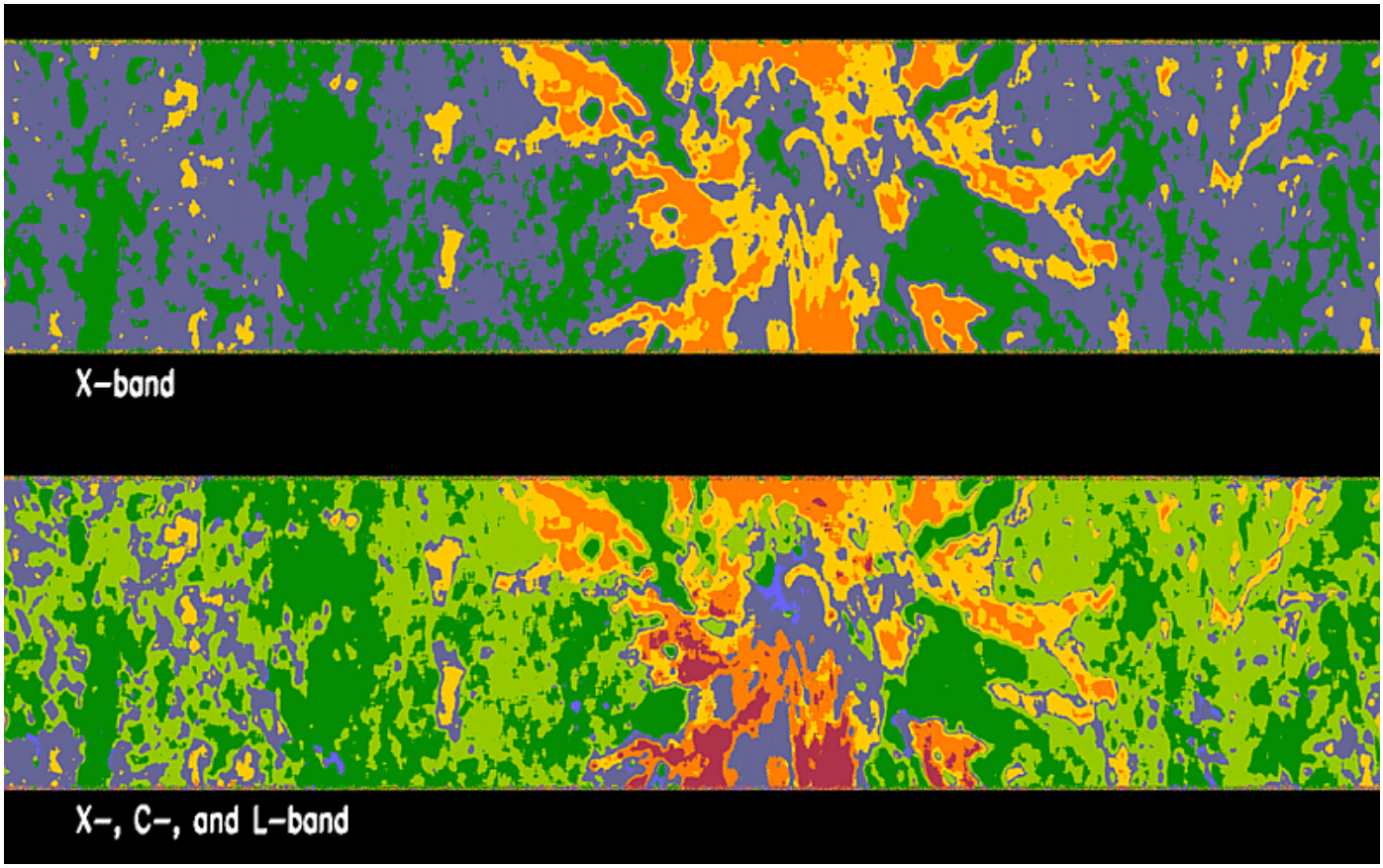

Figure 4: Coherence interpretation maps. Left: 4 classes interpretation based only on X-band. Right: 7 classes interpretation based on X-, C-, and L-band

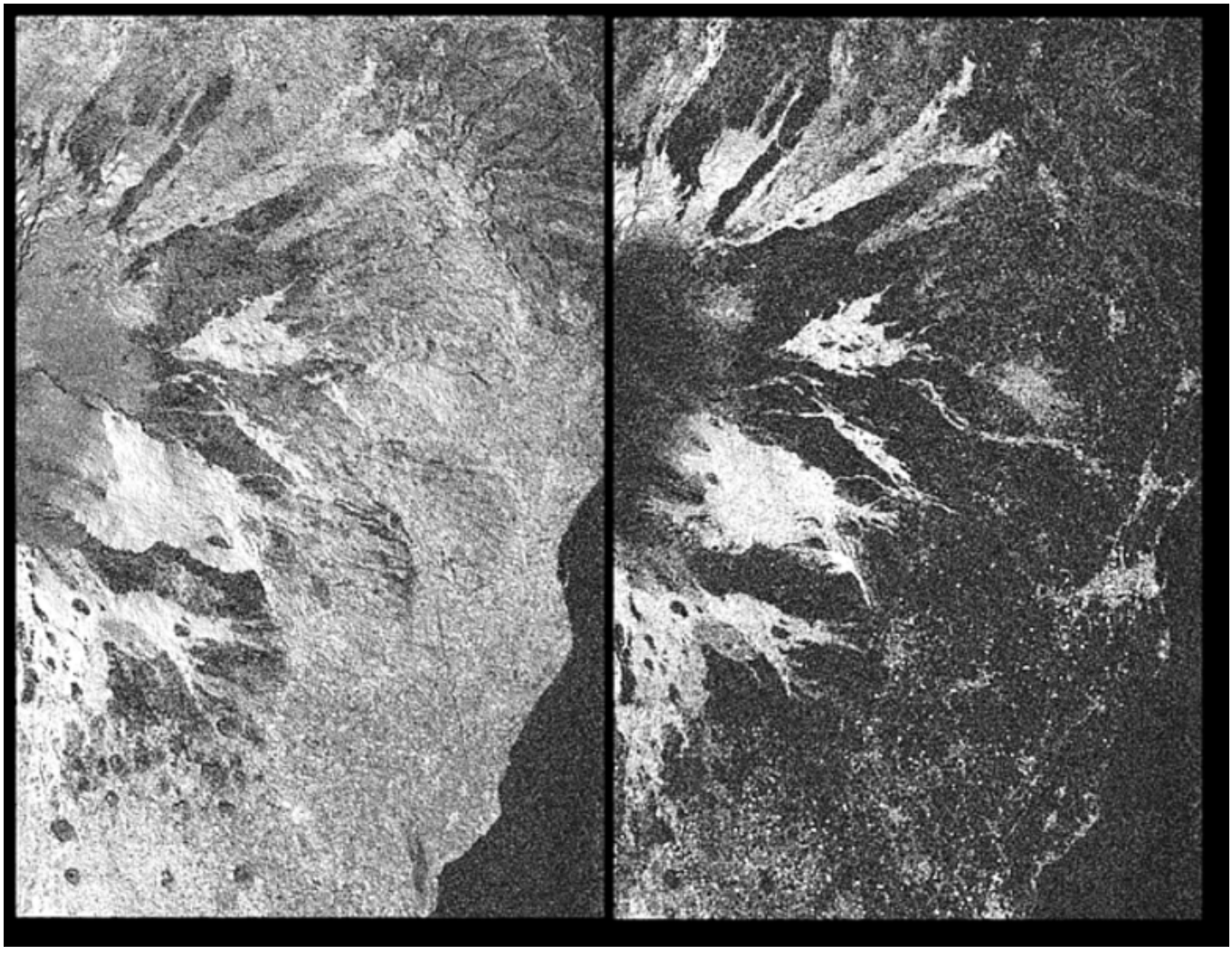

Figure 5: Coherence maps of the Mt. Etna area: 1-day coherence (left) and 70-days coherence (right)

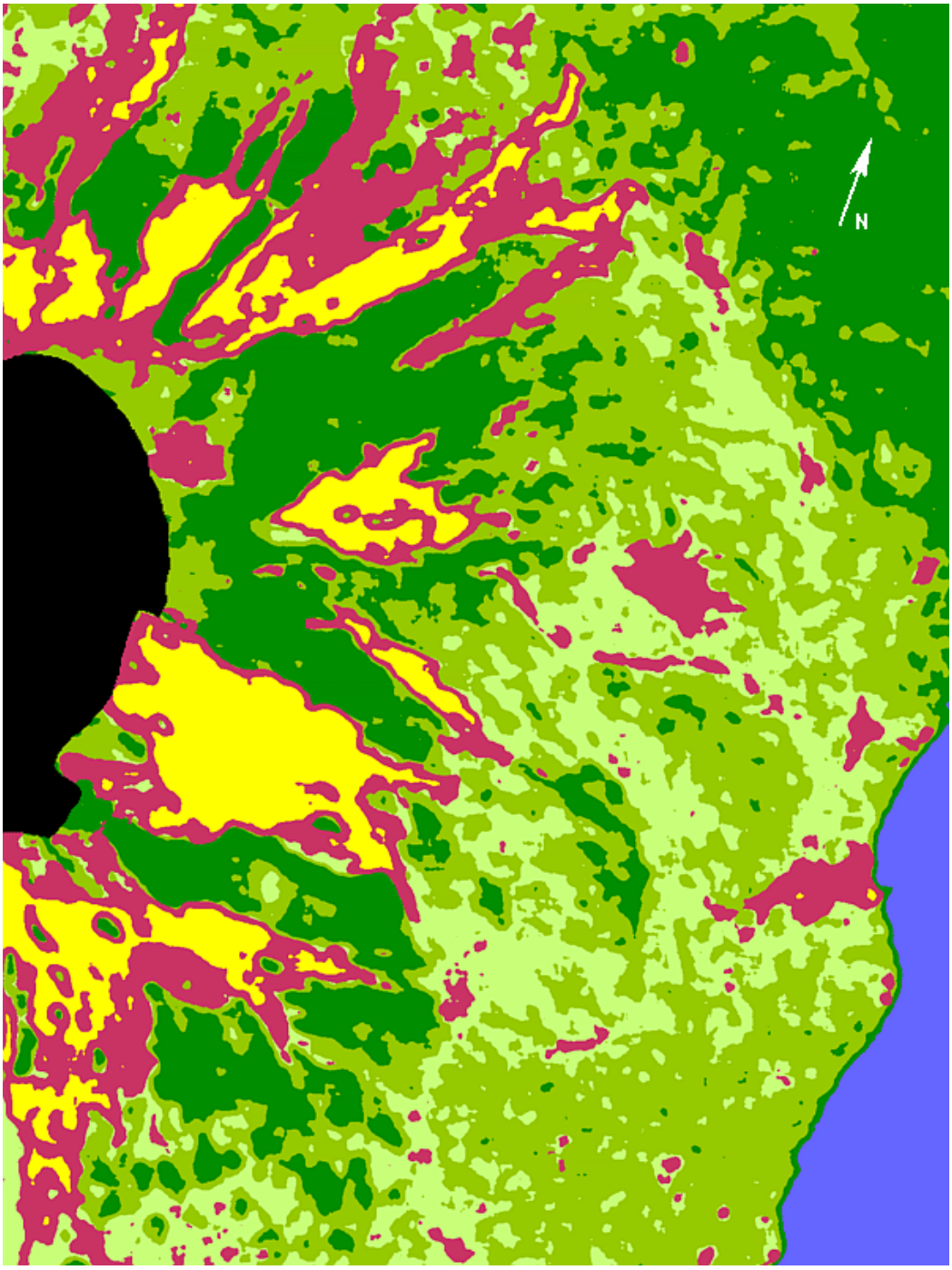

Figure 6: Multitemporal coherence interpretation map

References

[1] C. Prati, F. Rocca,
"Use of the Spectral Shift in SAR Interferometry", Proc. of the First ERS-1 Symposium, Cannes, pp. 691-696, November 1993.

[2] F. Gatelli, A. Monti-Guarnieri, F. Pasquali, C. Prati, F. Rocca,
"The Wavenumber Shift in SAR Interferometry", *IEEE Trans. on Geoscience and Remote Sensing, Vol. 32, No. 4, pp. 855-863, Juli 1994.*

[3] C. Prati, F. Rocca,
"Focusing SAR Data with Time-Varying Doppler Centroid", *IEEE Trans. on Geoscience and Remote Sensing, Vol. 30, No. 3, pp. 550-559, May 1992.*

[4] M. Schwäbisch, D. Geudtner,
"Improvement of Phase and coherence Map Quality Using Azimuth Prefiltering: Examples from ERS-1 and X-SAR", *Proc. of IGARSS'95}, Firence, pp. 205-207, 1995.*

[5] D. Fernandez, G. Waller, J.R. Moreira,
"Registration of SAR images using the chirp scaling algorithm", *Proc. of IGARSS'96, Lincoln, pp. 799-801, 1996.*

[6] R. Touzi, A. Lopes, J. Bruniquel, P. Vachon,
"Unbiased estimation of the coherence from multi-look SAR data", *IEEE Trans. on Geoscience and Remote Sensing, Vol. 68, No. 4, pp. 662-664, 1996.*

[7] S.G. Wells, J.C. Dohrenwend, L.D. McFadden, B.D. Turrin and K.D. Mahrer
"Late Cenozoid Landscape Evolution on Lava Flow Surfaces of the Clima Volcanic Field, Mojave Desert, California", *Geological Soc. Amer. Bulletin}, vol. 96, pp. 1518-1529, 1985.*